HHS Public Access

Author manuscript

Chem Res Toxicol. Author manuscript; available in PMC 2024 May 15.

Published in final edited form as:

Chem Res Toxicol. 2023 May 15; 36(5): 769–781. doi:10.1021/acs.chemrestox.3c00025.

Mass Spectrometry-based Metabolic Profiling of Urinary Metabolites of *N'*-Nitrosonornicotine (NNN) in the Rat

Yupeng Li[†,‡,*], **Romel P. Dator**[†], **Laura A. Maertens**[†], **Silvia Balbo**[†,§], **Stephen S. Hecht**[†]

[†] Masonic Cancer Center, University of Minnesota, Minneapolis, MN 55455

[‡] Department of Medicinal Chemistry, University of Minnesota, Minneapolis, MN 55455

[§] Division of Environmental Health Sciences, School of Public Health, University of Minnesota, Minneapolis, Minnesota 55455

Abstract

The tobacco-specific nitrosamines *N'*-nitrosonornicotine (NNN) and its close analog 4-(*N*-nitrosomethylamino)-1-(3-pyridyl)-1-butanone (NNK) are classified as "carcinogenic to humans" (Group 1) by the International Agency for Research on Cancer. The currently used biomarker to monitor NNN exposure is urinary total NNN (free NNN plus its *N*-glucuronide). However, total NNN does not provide information about the extent of metabolic activation of NNN as related to its carcinogenicity. Targeted analysis of the major metabolites of NNN in laboratory animals recently led to the identification of *N'*-nitrosonornicotine-1*N*-oxide (NNN-*N*-oxide), a unique metabolite detected in human urine that is specifically formed from NNN. To further investigate NNN urinary metabolites that hold promise as new biomarkers for monitoring NNN exposure, uptake, and/or metabolic activation, we conducted a comprehensive profiling of NNN metabolites in the urine of F344 rats treated with NNN or [pyridine-d_4]NNN. Using our optimized high-resolution mass spectrometry (HRMS)-based isotope-labeling method, 46 putative metabolites were identified with robust MS evidence. Out of the 46 candidates, all known major NNN metabolites were identified and structurally confirmed by comparing them to their isotopically labeled standards. More importantly, putative metabolites considered to be exclusively formed from NNN were also identified. The 2 new representative metabolites – 4-(methylthio)-4-(pyridin-3-yl)butanoic acid (**23**, MPBA) and *N*-acetyl-*S*-(5-(pyridin-3-yl)-1*H*-

[*]To whom correspondence should be addressed: Dr. Yupeng Li, Masonic Cancer Center and Department of Medicinal Chemistry, University of Minnesota, 2231 6th Street SE - 2-128 CCRB, Minneapolis, MN 55455, USA. phone: (612) 624-8187; lixx4803@umn.edu.

Conflict of Interest Disclosure

The authors declare no competing financial interest.

ASSOCIATED CONTENT

Supporting Information

The Supporting Information is available free of charge on the ACS Publications website at www.acs.org:

NMR spectra of compounds **23** and **24** (Figures S1 and S2); experimental protocol of the NNN metabolism rat study (Figure S3); proposed mostly likely structures of matched d_0–d_4 peak pairs observed in the rat urine (Figure S4); MS^2 fragmentation patterns of matched d0-d4 peak pairs observed in the rat urine (Figure S5); MS^2 and MS^3 fragmentation patterns of putative metabolites specifically formed by NNN in the rat urine (Figure S6); spiking experiments of **23** and **24** in the U1* of rats #1 and #3; body weight of F344 rats and their dosing records (Table S1); result of untargeted MS full scan of NNN-treated rat urine (Table S2) and matched d_0–d_4 peak pairs in the U1* (Table S3) and U2* (Table S4) of rats (separate Excel files); putative NNN metabolites in the U1* (Table S5) and U2* (Table S6) of rats treated with d_0- or d_4-NNN; distribution pattern of 7 putative metabolites that are considered to be specifically formed by NNN in the rat urine (Table S7); proposed mechanism of formation of compounds **23** and **24** (Scheme S1).

pyrrol-2-yl)-L-cysteine (**24**, Py-Pyrrole-Cys-NHAc) – were identified by comparing them to synthetic standards that were fully characterized by NMR and HRMS. They are hypothesized to be formed by NNN α-hydroxylation pathways and thus represent the first potential biomarkers to specifically monitor the uptake plus metabolic activation of NNN in tobacco users.

Graphical Abstract

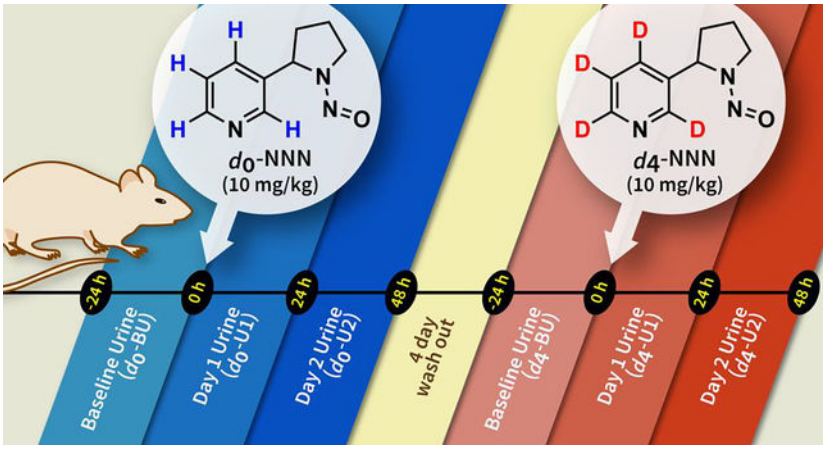

INTRODUCTION

Since its first identification in tobacco smoke and unburned tobacco in the 1970s,[1,2] *N*′-nitrosonornicotine (**1**, NNN, Scheme 1) has been consistently quantified as one of the most abundant *N*-nitrosamine carcinogens in tobacco products.[3] In one recent study, NNN occurred at a mean level of 1900.7 ± 359 ng/g in cigarette tobacco filler and 85 ± 31 ng/cigarette in the mainstream smoke (with the ISO machine-smoking regimen) of 50 U.S. domestic cigarette products.[4] Its concentration (median: 446 ng/cigar; ranging from 201 to 1450 ng/cigar) was ~5 times higher in the mainstream smoke of 60 U.S. commercial little cigars.[5] NNN occurred in much higher levels in some smokeless tobacco products such as Zarda and Gul from South-East Asia, amounting to 2.8–59 μg/g tobacco powder.[6,7] These concentrations significantly exceed the maximum level of NNN (1 μg/g dry tobacco weight) in any batch of finished smokeless tobacco products proposed by the U.S. Food and Drug Administration.[8]

The ability of NNN to cause tumors in the esophagus, oral cavity, nasal cavity, lung and trachea has been well documented in laboratory animal studies.[9] Multiple epidemiology studies in South-East Asia demonstrated an increased risk of oral and pharyngeal cancers in smokeless tobacco users living there.[10–13] A positive association between smokeless tobacco use and an increased risk of oral cancer and esophageal cancer incidence was also observed in studies conducted in the U.S. and some of the South-East Asian countries.[10,12] A recent review of smokeless tobacco products consumed in South-East Asian countries and oral cancer risk concluded that products with higher NNN concentrations pose higher cancer risks.[14] On the basis of laboratory studies, epidemiology data, and an understanding of metabolic activation pathways, NNN and the closely related carcinogen

4-(*N*-nitrosomethylamino)-1-(3-pyridyl)-1-butanone (NNK) together have been classified as "carcinogenic to humans" (Group 1) by the International Agency for Research on Cancer.[15]

To monitor human exposure to NNN, the currently applied biomarker is urinary "total NNN" that is composed of free NNN plus its *N*-glucuronide (**5**, NNN-*N*-Gluc). The levels of total NNN were strongly associated with esophageal cancer risk in cigarette smokers of the Shanghai Cohort study.[16] However, total NNN has some drawbacks. The levels of urinary free NNN are relatively low, requiring extensive precautions to avoid its artifactual formation by nitrosation of nornicotine – a tobacco alkaloid constituent and nicotine metabolite that is present in relatively high abundance in urine.[17] Thus, It is important to identify a urinary metabolite that specifically results from NNN metabolism, with the potential to be an improved biomarker for monitoring the uptake of NNN and possibly its metabolic activation in tobacco users.

The metabolism pathways of NNN have been extensively investigated (Scheme 1).[18] In the urine of rats, mice and Syrian golden hamsters, the major metabolites of NNN were 4-hydroxy-4-(pyridin-3-yl)butanoic acid (hydroxy acid, **19**, 37.1 – 53.3% of the dose), 4-oxo-4-(pyridin-3-yl)butanoic acid (keto acid, **18**, 12.8 – 31.1%), *N*′-nitrosonornicotine-1*N*-oxide (NNN-*N*-oxide, **6**, 6.7 – 10.7%), and norcotinine **8** (3.2 – 5.1%), measured together with the unmodified NNN **1** (3.3 – 5.2%).[19–21] In the urine of a patas monkey intravenously administered [5-^{3}H]NNN, hydroxy acid **19** was the major metabolite (43.8 ± 4.0%), followed by 3′-hydroxynorcotinine **9** (16.9%), norcotinine-1*N*-oxide **12** (16.5%), norcotinine **8** (13.1%), 3′-(*O*-β-D-glucopyranuronosyl)hydroxynorcotinine **13** (5.4%) and keto acid **18** (2.7%).[22] It would be ideal to use the major metabolites such as hydroxy acid **19**, keto acid **18** and norcotinine **8** (and its derivatives **9**, **12** and **13** as observed in the patas monkey) as urinary biomarkers to monitor NNN exposure. However, they can all result from nicotine metabolism as minor metabolites, and there is at least 10,000 times greater concentrations of nicotine than NNN in tobacco products; thus, even minor nicotine metabolites are found in far greater concentrations in urine than the same metabolites formed from NNN.[23] Hydroxy acid **19** and keto acid **18** are also the principal metabolites of NNK, which always occurs together with NNN in tobacco products and is a potent lung carcinogen.[3,18] NNN-*N*-oxide **6** has structural specificity to NNN metabolism and was one of the most abundant metabolites in rat urine.[19] However, it was not observed in the urine and serum of the patas monkey.[22] We recently reported the first identification of NNN-*N*-oxide in the urine of cigarette smokers and smokeless tobacco users.[24] The levels of NNN-*N*-oxide were near the quantitation limit in the urine of cigarette smokers, amounting to a mean of 8.40 ± 6.04 fmol/mL urine with a detection rate of 31.2%.

Therefore, in an effort to identify potential urinary biomarkers that are exclusively formed from NNN, we took advantage of the high-resolution mass spectrometry (HRMS)-based stable-isotope labeling method that we have developed.[25] We conducted a comprehensive profiling of NNN metabolites in the urine of rats administered NNN or [pyridine-d_4]NNN by gavage, recognizing that newly identified metabolites most likely will be quantitatively minor ones. The workflow of sample purification and high-performance liquid chromatography-mass spectrometry (HPLC-MS) and data analysis was optimized to process a substantial number of possible candidate metabolites. Structures of the candidates were

proposed based on the evidence of their corresponding MS^2 and MS^3 spectra. Among these, most of the known major NNN metabolites were detected and structurally confirmed by co-elution with their isotopically labeled standards. Previously known metabolites from our NNK metabolic profiling study[25] including **14**, **21** and **22** were identified as new metabolites of NNN in this study. Seven putative metabolites identified with strong MS^2 and MS^3 evidence were considered to be formed specifically in NNN metabolism. Structures of the 2 representative compounds – 4-(methylthio)-4-(pyridin-3-yl)butanoic acid (**23**, MPBA, Figure 1) and *N*-acetyl-*S*-(5-(pyridin-3-yl)-1*H*-pyrrol-2-yl)-L-cysteine (**24**, Py-Pyrrole-Cys-NHAc) – were verified by comparing them to their fully characterized synthetic standards. They are hypothesized to be formed by NNN α-hydroxylation pathways and thus represent potential biomarkers to monitor the uptake plus metabolic activation of NNN in tobacco users.

MATERIALS AND METHODS

Caution:

NNN is highly carcinogenic. It should be handled in a well-ventilated fume hood with extreme caution and with appropriate protective equipment.

Chemicals and supplies:

Racemic NNN was previously synthesized[26] with a purity of >99% after HPLC purification. Racemic [pyridine-d_4]NNN was purchased from Toronto Research Chemicals (Ontario, Canada). The other isotopically-labeled standards including [CH_2-d_4]HPB, [$^{13}C_6$]NNN, [pyridine-d_4]NNN-*N*-oxide, [pyridine-d_4]keto acid, and [$^{13}C_6$]hydroxy acid were synthesized during our previous studies.[17,24,27,28] [pyridine-d_4]Norcotinine was generously provided by Dr. Sharon Murphy's laboratory. Phosphate buffered saline (PBS, 10X) was purchased from Invitrogen (Grand Island, NY) and diluted to 1X before use. Recombinant β-glucuronidase from *Escherichia coli* (catalog # G8295, ≥ 10,000,000 units/g protein, lyophilized powder) was procured from Sigma-Aldrich (St. Louis, MO). Strata™-X 33 μm Polymeric Reversed Phase cartridges (30 mg/1 mL, 100/pk, catalog # 8B-S100-TAK) were purchased from Phenomenex (Torrance, CA). Oasis MCX 3 cc (60 mg) LP Extraction Cartridges (Part # 186000253, 100/pk) and Oasis PRiME HLB 3 cc (60 mg) Extraction Cartridges (Part # 186008056, 100/pk) were obtained from Waters (Milford, MA). Titan syringe filter (PTFE, 0.2 μm, 4 mm, 100/pk, catalog # 42204-NP, lot # 00287675) was purchased from Thermo Fisher Scientific (Waltham, MA). Silanized 4 mL glass vials (catalog # CTV-7472) and glass vials with 300 μL fused inserts (catalog # CP-0952–03SIL) were purchased from Chrom Tech (Apple Valley, MN). All other chemicals and supplies were procured from Sigma-Aldrich or Thermo Fisher Scientific. Milli-Q water (Millipore) was routinely used unless otherwise noted.

Synthesis of chemical standards:

MPBA (**23**) and Py-Pyrrole-Cys-NHAc (**24**) were synthesized as shown in Scheme 2. Both compounds were synthesized under contract by Wuxi AppTech (Shanghai, China); compound **23** was also synthesized independently in our laboratory.

Methyl 4-hydroxy-4-(pyridin-3-yl)butanoate (26).—Compound **25** was synthesized using the method previously reported.[29] To a solution of **25** (1.0 g, 5.58 mmol) in THF (6.0 mL) was added $NaBH_4$ (253 mg, 6.70 mmol) at 0 °C. The reaction mixture was stirred at 25 °C for 2 h and worked up by addition of 1 N HCl at 0 °C to adjust pH to 5–6. The resulting mixture was extracted with dichloromethane (DCM) 3 times. The organic phases were combined, washed with brine, dried with Na_2SO_4, and concentrated under vacuum. The resulting residue was purified by silica gel flash column chromatography (hexanes/EtOAc) to afford **26** as a white solid (0.8 g, 79.1%). ^{1}H NMR (500 MHz, $CDCl_3$) δ 8.60 – 8.55 (m, 1H), 8.47 (d, *J* = 5.4 Hz, 1H), 7.94 (dt, *J* = 7.9, 1.8 Hz, 1H), 7.48 (dd, *J* = 8.0, 5.6 Hz, 1H), 4.88 (dd, *J* = 8.5, 4.0 Hz, 1H), 3.69 (s, 3H), 2.59 – 2.40 (m, 2H), 2.12 – 2.04 (m, 1H), 2.04 – 1.95 (m, 1H). The side products 1-(pyridin-3-yl)butane-1,4-diol (1,4-diol, **14**) and 5-(3-pyridyl)-2-hydroxytetrahydrofuran (lactol, **17**) were also isolated and confirmed by ^{1}H NMR.

Methyl 4-((methylsulfonyl)oxy)-4-(pyridin-3-yl)butanoate (27).—To a solution of **26** (90 mg, 0.46 mmol) and Et_3N (96 μL, 0.69 mmol) in DCM (2.0 mL) was added methanesulfonyl chloride (43 μL, 0.55 mmol) at 0 °C. The reaction mixture was stirred at 0 °C for 0.5 h, then evaporated to dryness; the residue was purified by silica gel flash column chromatography (hexanes/EtOAc) to afford **27** as a colorless oil (87 mg, 69.2%). ^{1}H NMR (500 MHz, $CDCl_3$) δ 8.67 (t, *J* = 1.4 Hz, 1H), 8.62 (d, *J* = 5.7 Hz, 1H), 7.98 (d, *J* = 8.0 Hz, 1H), 7.57 (dd, *J* = 8.0, 5.6 Hz, 1H), 5.75 (dd, *J* = 8.9, 4.7 Hz, 1H), 3.71 (s, 3H), 3.01 (d, *J* = 0.7 Hz, 3H), 2.63 – 2.42 (m, 2H), 2.35 – 2.18 (m, 2H).

Methyl 4-(methylthio)-4-(pyridin-3-yl)butanoate (28).—To a solution of **27** (273 mg, 1 mmol) in THF (2.0 mL) was added sodium thiomethoxide (85 mg, 1.2 mmol). The reaction mixture was stirred at 50 °C for 1.5 h, then diluted in H_2O and extracted with EtOAc 3 times. The organic phases were combined, dried with Na_2SO_4, and concentrated under vacuum. The resulting residue was purified by silica gel flash column chromatography (hexanes/EtOAc) to afford **28** as a colorless oil (84 mg, 37.3%). An alternative method was also used to synthesize **28** by reacting the intermediate **26** with dimethyl disulfide and tributylphosphine in THF. To a solution of **26** (215 mg, 1.10 mmol) in THF (2.5 mL) was added dimethyl disulfide (239 μL, 2.65 mmol) and tributylphosphine (354 μL, 1.43 mmol). The reaction mixture was stirred at 25 °C for 2 h. The mixture was concentrated to dryness and the resulting residue was purified by silica gel flash column chromatography (DCM/MeOH) to afford **28** as a yellow oil (0.1 g, 40.2%). ^{1}H NMR (500 MHz, $CDCl_3$) δ 8.48 (s, 1H, pyr-H_2), 8.47 (d, *J* = 5.3 Hz, 1H, pyr-H_6), 7.92 (d, *J* = 8.0 Hz, 1H, pyr-H_4), 7.48 (dd, *J* = 8.0, 5.6 Hz, 1H, pyr-H_5), 3.75 (t, *J* = 7.6 Hz, 1H, pyr-C<u>H</u>-), 3.63 (s, 3H, -COOC<u>H_3</u>), 2.40 (t, *J* = 7.4 Hz, 2H, -C<u>H_2</u>-$COOCH_3$), 2.24 – 2.04 (m, 2H, -C<u>H_2</u>-CH_2-$COOCH_3$), 1.86 (s, 3H, -SC<u>H_3</u>). ^{1}H NMR (500 MHz, DMSO-*d*$_6$) δ 8.58 – 8.50 (m, 1H, pyr-H_2), 8.49 (d, *J* = 5.6 Hz, 1H, pyr-H_6), 8.14 (dt, *J* = 8.1, 1.7 Hz, 1H, pyr-H_4), 7.70 (dd, *J* = 8.0, 5.6 Hz, 1H, pyr-H_5), 4.01 (t, *J* = 7.6 Hz, 1H, pyr-C<u>H</u>-), 3.55 (s, 3H, -COOC<u>H_3</u>), 2.43 – 2.26 (m, 2H, -C<u>H_2</u>-$COOCH_3$), 2.21 – 2.05 (m, 2H, -C<u>H_2</u>-CH_2-$COOCH_3$), 1.86 (s, 3H, -SC<u>H_3</u>). ^{13}C NMR (126 MHz, DMSO-*d*$_6$) δ 172.36 (-<u>C</u>$OOCH_3$), 146.21 (pyr-C_2), 145.94 (pyr-C_6), 140.65 (pyr-C_3), 138.75 (pyr-C_4), 126.10 (pyr-C_5), 51.36 (-COO<u>C</u>H_3), 45.71 (pyr-<u>C</u>H-),

31.33 (-$\underline{C}H_2$-$COOCH_3$), 29.23 (-$\underline{C}H_2$-CH_2-$COOCH_3$), 13.09 (-S$\underline{C}H_3$). HRMS $[M + H]^+$: calc'd 226.0896; found: 226.0900.

4-(Methylthio)-4-(pyridin-3-yl)butanoic acid (23, MPBA).—A solution of **28** (52 mg, 0.18 mmol) and LiOH (6.5 mg, 0.27 mmol) in THF (0.5 mL) and H_2O (0.5 mL) was stirred at room temperature overnight. Most of the solvents were evaporated and the resulting solution was adjusted to pH 6 using 0.1 N HCl. The mixture was subjected to reverse phase HPLC using an 8-min isocratic method with 80% MeOH. The peak at 4.5 min was collected and dried to afford **23** as a colorless oil (24.4 mg, 60.2%). NMR spectra of **23** are presented in Supplementary Figure S1. ^{1}H NMR (500 MHz, $CDCl_3$) δ 8.45 (s, 1H, pyr-H_2), 8.44 (d, J = 5.5 Hz, 1H, pyr-H_6), 7.95 (d, J = 8.0 Hz, 1H, pyr-H_4), 7.49 (dd, J = 8.0, 5.6 Hz, 1H, pyr-H_5), 3.77 (t, J = 7.5 Hz, 1H, pyr-C$\underline{H}$-), 2.39 – 2.22 (m, 2H, -C$\underline{H}_2$-COOH), 2.13 – 1.98 (m, 2H, -C$\underline{H}_2$-CH_2-COOH), 1.82 (s, 3H, -SC$\underline{H}_3$). ^{1}H NMR (600 MHz, DMSO-d_6) δ 12.17 (s, 1H, -COOH), 8.85 (d, J = 2.1 Hz, 1H, pyr-H_2), 8.80 (dd, J = 5.6, 1.3 Hz, 1H, pyr-H_6), 8.49 (dt, J = 8.2, 1.6 Hz, 1H, pyr-H_4), 7.98 (dd, J = 8.1, 5.4 Hz, 1H, pyr-H_5), 4.08 (t, J = 7.6 Hz, 1H, pyr-CH-), 2.32 (ddd, J = 16.4, 8.5, 6.4 Hz, 1H, -C$\underline{H}_2$-COOH), 2.25 (ddd, J = 16.5, 8.0, 6.5 Hz, 1H, -C$\underline{H}_2$-COOH), 2.21 – 2.05 (m, 2H, -C$\underline{H}_2$-CH_2-COOH), 1.88 (s, 3H, -SCH_3). ^{13}C NMR (151 MHz, DMSO-d_6) δ 173.48 (-COOH), 143.58 (pyr-C_4), 141.82 (pyr-C_3), 141.62 (pyr-C_2), 141.52 (pyr-C_6), 126.85 (pyr-C_5), 45.76 (pyr-$\underline{C}$H-), 31.55 (-$\underline{C}H_2$-COOH), 29.11 (-$\underline{C}H_2$-CH_2-COOH), 13.10 (-SCH_3). HRMS $[M + H]^+$: calc'd 212.0740; found: 212.0741.

3-(5-Bromo-1H-pyrrol-2-yl)pyridine (30).—The starting material β-nornicotyrine (**29**) was purchased from Toronto Research Chemicals (Ontario, Canada, catalogue No. #N825000); it can also be synthesized as reported.[30] To a solution of **29** (0.20 g, 1.39 mmol) in *N*,*N*-dimethylformamide (DMF, 1.0 mL) was added *N*-iodosuccinimide (343 mg, 1.53 mmol) at −10 °C. The reaction mixture was stirred at 0 °C for 2 h. The resulting mixture was evaporated to dryness and the residue was purified by reverse phase HPLC using a Phenomenex Luna C18 column (80 × 30 mm; 3 μm). The mobile phase was (A) H_2O with 0.1% HCl and (B) CH_3CN. An 8-min linear gradient starting from 10% to 40% B was used. The desired product was obtained as a white solid (15 mg, 4.0%) along with the formation of the other major side products 4′-iodo-β-nornicotyrine and 4′, 5′-diiodo-β-nornicotyrine. ^{1}H NMR (400 MHz, $CDCl_3$) δ 8.94 (br s, 1H), 8.60 (br d, J = 8.4 Hz, 1H), 8.38–8.49 (m, 1H), 7.91 (dd, J = 8.0, 5.9 Hz, 1H), 6.77 (d, J = 3.6 Hz, 1H), 6.40 (d, J = 3.6 Hz, 1H). MS $[M + H]^+$: calc'd 271.0; found: 271.0.

N-Acetyl-S-(5-(pyridin-3-yl)-1H-pyrrol-2-yl)-L-cysteine (24, Py-Pyrrole-Cys-NHAc).—To a solution of **30** (50 mg, 0.185 mmol) and Et_3N (51.5 μL, 0.37 mmol) in DMF (0.35 mL) was added *N*-acetyl-L-cysteine **31** (30.2 mg, 0.185 mmol). The reaction mixture was stirred at 90 °C for 3 h. The solvents were evaporated and the resulting residue was purified by reverse phase HPLC using a Phenomenex Luna C18 column (75 × 30 mm; 3 μm). The mobile phase was (A) H_2O with NH_4HCO_3 and (B) CH_3CN. A 10-min linear gradient starting from 1% to 25% B was used. Compound **24** was obtained as a yellow solid (3.7 mg, 7.1%). NMR spectra of **24** are presented in Figure S2. ^{1}H NMR (500 MHz, DMSO-d_6) δ 12.27 (s, 1H, -COOH), 9.77 – 8.66 (m, 1H, pyr-H_2), 8.35 (d, J

= 4.6 Hz, 1H, pyr-H_6), 8.16 – 7.63 (m, 2H, -CONH- and pyr-H_4), 7.37 (dd, J = 8.1, 4.7 Hz, 1H, pyr-H_5), 6.64 (dd, J = 3.6, 2.1 Hz, 1H, pyrrole-$H_{4'}$), 6.25 (dd, J = 3.6, 1.7 Hz, 1H, pyrrole-$H_{3'}$), 4.61 – 3.94 (m, 1H, -CH(NHAc)COOH), 3.08 (dd, J = 13.4, 4.6 Hz, 1H, -SCH_2-), 2.84 (dd, J = 13.4, 7.9 Hz, 1H, -SCH_2-), 1.87 (s, 3H, -$COCH_3$). ^{1}H NMR (600 MHz, DMSO-d_6) δ 12.20 (s, 1H, -COOH), 8.91 (d, J = 2.4 Hz, 1H, pyr-H_2), 8.36 (dd, J = 4.8, 1.5 Hz, 1H, pyr-H_6), 8.06 (s, 1H, -CONH-), 8.01 (dt, J = 8.0, 2.0 Hz, 1H, pyr-H_4), 7.37 (dd, J = 8.0, 4.7 Hz, 1H, pyr-H_5), 6.87 – 6.57 (m, 1H, pyrrole-$H_{4'}$), 6.26 (t, J = 2.9 Hz, 1H, pyrrole-$H_{3'}$), 4.23 (s, 1H, -CH(NHAc)COOH), 3.09 (dd, J = 13.5, 4.7 Hz, 1H, -SCH_2-), 2.86 (dd, J = 13.5, 8.0 Hz, 1H, -SCH_2-), 1.87 (s, 3H, -$COCH_3$). ^{13}C NMR (151 MHz, DMSO-d_6) δ 171.83 (-COOH), 169.31 (-$NHCOCH_3$), 146.70 (pyr-C_6), 144.93 (pyr-C_2), 130.73 (pyrrole-$C_{2'}$), 130.23 (pyr-C_4), 128.07 (pyr-C_3), 123.73 (pyr-C_5), 121.08 (pyrrole-$C_{5'}$), 117.99 (pyrrole-$C_{3'}$), 107.63 (pyrrole-$C_{4'}$), 53.36 (-CHNH-), 40.04 (-SCH_2-), 22.62 (-$COCH_3$). HRMS $[M + H]^+$: calc'd 306.0907; found: 306.0903.

NNN metabolism in F344 rats:

This study was approved by the University of Minnesota Institutional Animal Care and Use Committee (Protocol # 1906-37182A). The experimental protocol is illustrated in Figure S3. Three male F344 rats (163.7 ± 7.5 g, Charles River Laboratories, Kingston, NY) were housed under standard conditions for 5 days. They were acclimated to metabolism cages by increasing time intervals of 2, 4 and 6 h for the first 3 days and returned to normal cages for the following 2 days. The 3 rats were then moved to the metabolism cages and the 24 h baseline urine (d_0-BU) samples were collected. On the next day, NNN (10 mg/kg body weight) in H_2O (265 μL) was administered by gavage, and the 24 h urine (d_0-U1) and the next 24 h urine (d_0-U2) were collected. The rats were moved back to the regular housing conditions for 4 days with an additional acclimation time of 6 h in the metabolism cage on the 4th day. Following the same protocol, the d_4-BU was collected prior to [pyridine-d_4]NNN administration (10 mg/kg body weight) and d_4-U1 and d_4-U2 post dosing were collected. All the urine samples were collected in a cooled environment (~4 °C) provided by the chillers associated with the metabolism cages. Urine samples (4–5 mL each) were stored at −20 °C until analysis. There was no body weight loss caused by NNN administration (Table S1). All the rats were euthanatized with CO_2 at the end of this study and the tissues were harvested for future use.

Rat urine preparation:

For each rat, the NNN and [pyridine-d_4]NNN urine samples from the same time points were combined (0.1 mL each) in a 1:1 ratio and diluted in 0.8 mL PBS buffer (pH = 7). These samples were labeled as BU* (d_0- plus d_4-BU), U1* (d_0- plus d_4-U1), and U2* (d_0- plus d_4-U2), respectively. A PBS control sample was also included in the analysis. All the samples were purified using our previous protocol[25] with some modifications.

The urine mixtures (and the PBS control sample) were incubated with β-glucuronidase (5000 units) at 37 °C overnight. After incubation, the internal standard [$^{13}C_6$]NNN (500 pg, 2.72 pmol) was spiked into the mixtures before adding 2.0 mL of CH_3CN/MeOH/acetone (1:1:1 by volume). The solution was vortexed and incubated for 15 min on ice. The solution was centrifuged (14,000 r.p.m., 4 °C, 10 min) and the supernatant was collected and

dried with a SpeedVac. Using the same solid-phase extraction (SPE) method as described previously,[25] the fraction after the SPE steps with Oasis HLB cartridges (3 mL of MeOH), Oasis MCX cartridges (1.8 mL of MeOH containing 1% NH_4OH), and Strata-X cartridges (1 mL of MeOH) was dried and reconstituted in 100 μL 10% CH_3CN (Optima®) in H_2O (Optima®) and transferred to a glass vial with a 300 μL insert vial. The solvent was evaporated with a SpeedVac. The dried residue was re-dissolved in 50 μL of H_2O (Optima®) and filtered via syringe filter (Thermo Scientific) prior to MS analysis.

LC-MS parameters:

An aliquot of 1 μL of worked up urine was analyzed using a Dionex UltiMate 3000 RSLCnano UPLC system coupled to a Thermo Scientific™ Orbitrap Fusion Lumos Tribrid Mass Spectrometer with a Nanospray Flex ion source (Thermo Fisher Scientific, San Jose, CA). Chromatographic separation was performed using a custom-packed capillary column (75 μm i.d., ~20 cm length, 10 μm orifice) containing a fused-silica emitter (New Objective, Woburn, MA) with 5 μm particle size Luna C18 stationary phase (Phenomenex, Torrance, CA). The mobile phase consisted of (A) 5 mM NH_4OAc (Optima®) and (B) MeOH (Optima®).

A 35-min program was used with a gradient starting from 5% B at a flow rate of 1 μL/min for 5 min. This was followed by switching the injection valve to remove the sample injection loop (5 μL) from the flow path and reducing the flow rate to 0.3 μL/min over 1 min. While keeping the flow rate at 0.3 μL/min, the gradient was increased linearly to 98% B over 19 min, followed by holding at 98% B for 3 min before returning to 5% B in 2 min. The flow rate was then increased to 1 μL/min in 2 min. The instrument was equilibrated for 3 min at the initial conditions before the next injection.

MS analysis was performed in the positive ion profile mode with a 2.2 kV spray voltage and a 300 °C ion transfer tube temperature. The S-lens RF setting (%) was 60. The number of micro-scans was set at 1. The EASY-IC™ internal mass calibration feature was used to ensure maximum mass accuracy. Extraction of precursor ion signals and product ion signals was performed with less than 5 ppm mass tolerance. Thermo Xcalibur Qual Browser (version 4.3.73.11) was used to process all the MS data.

Untargeted MS full scan analysis of rat urine:

Using a similar approach as described in our previous study,[25] an untargeted full scan was first conducted for screening NNN metabolites in all the 3 urine mixtures and the PBS control. The parameters for the untargeted full scan were: Orbitrap resolution, 240,000; scan range, *m/z* 100–500 using quadrupole isolation; AGT target, standard; injection time, 100 ms; data type, centroid. After acquisition of the full scan data, feature analysis using Compound Discoverer 3.2 (Thermo Fisher Scientific) was conducted with the same criteria as used before.[25] The resulting features were exported to Microsoft® Excel® 2016 (Microsoft, Redmond, WA). For each feature, 3 parameters were evaluated, including *m/z*, retention time (t_R) and peak area using an updated version of the custom JAVA script (Supplementary material) we have developed previously.[25] The updated version allows us to process a significantly increased number of features. Any feature presenting a pair with an

m/z difference of 4.0251 ± 0.001 Da and a t_R difference of 0.2 min and the peak area ratio of 0.1–10 was considered (Table 1). The matched d_0–d_4 pairs in the U1* and U2* samples of each rat were then combined and the redundant peaks (including potential isomers) as well as the peaks that were present in the PBS and BU* samples were removed. The list of the remaining d_0–d_4 pairs was further shortened by removing any matched pairs with $t_R \leq$ 5 min. The total numbers of the matched d_0–d_4 pairs after the untargeted MS analysis were 285, 228 and 206 for rat #1, #2 and #3, respectively. The exact mass, t_R and peak area of these matched d_0–d_4 pairs as well as their distribution pattern in the rat urines are presented in Table S2.

Targeted MS^2 analysis of matched d_0–d_4 peak pairs:

For structural assignment of the matched d_0–d_4 peak pairs, targeted MS^2 analysis was needed. Among the total number of 397 matched d_0–d_4 peak pairs detected in all 3 rats (Table S2), 161 pairs were of particular interest due to their higher occurrence frequency in the U1* of at least 2 rats (Figure 2A). There were 31 matched d_0–d_4 peak pairs observed in the U2* of at least 2 rats (Figure 2B).

Due to the limit of the MS analytical power, simultaneous targeted MS^2 analysis of the 161 d_0–d_4 pairs would be difficult to generate informative data especially for those with low urinary abundance and/or MS response. We thus undertook a strategy of sorting the peak pairs into 8 subgroups based on their mass area of the d_0 peak in the U1* samples. As shown in Table S3, each subgroup contains 24 – 45 of analytes with their MS areas relatively close to each other. The collision type used for the MS^2 fragmentation was higher-energy collisional dissociation (HCD) at 30%. The other MS parameters of Orbitrap resolution and injection time (ms) for each individual subgroup are also included in Sheet 3 of Table S3. For low abundant d_0–d_4 pairs, a 2nd round of targeted MS^2 analysis was conducted using the same subgrouping approach. The peak pairs and MS parameters are shown in Sheet 4 of Table S3.

For the 31 matched d_0–d_4 pairs of interest in the U2* samples, only 5 pairs were uniquely present with no occurrence in the U1* collections (Table S4, Sheet 1). There were 3 additional pairs of interest due to their presence in U1* of only one rat. These 8 matched d_0–d_4 pairs were similarly subjected to the targeted MS^2 analysis with the key MS parameters including Orbitrap resolution set to 30000 and injection time of 100 ms are shown in Sheet 2 of Table S4. The collision type for MS^2 fragmentation was HCD at 30%.

After acquisition of the targeted MS^2 scan data, each matched d_0–d_4 pair was examined manually using Xcalibur Qual Browser 4.2 (Thermo Scientific) to ensure similar t_R, peak shapes and intensities. Peaks considered to be candidates were those with at least 2–3 MS^2 fragment ions for both d_0 and d_4 *m/z* values. As summarized in Table S5, in the U1* of rats, nearly 2/3 of the 161 matched d_0–d_4 pairs were not identified with required peak features by the targeted MS^2 analysis. Some of the pairs were characterized to be in-source-decay ions from some abundant metabolites such as NNN-*N*-oxide; some were interfering peaks due to the relatively broad MS^2 isolation window (*m/z* 1.5); clusters and dimers were also observed. A similar result was also observed in the U2* of rats (Table S6).

Out of the 161 matched d_0–d_4 pairs, we identified 44 to be putative NNN metabolites in the U1* of rats; out of the 31 matched d_0–d_4 pairs, we identified 2 additional pairs to be putative NNN metabolites in the U2* of rats. Their most likely structures are proposed and described in Table 2 (with entries #3 and #22 being the U2*-unique metabolites) and Figure S4. The MS^2 fragmentation patterns of these putative NNN metabolites are presented in Figure S5.

Targeted MS^2 and MS^3 analysis of putative NNN-specific metabolites:

Among the 46 putative metabolites of NNN (Table 2), compounds that would likely be specifically formed from NNN were of greater interest because they could be used as potential biomarkers to monitor NNN metabolic activation in tobacco users. Thus, further structural analysis using targeted MS^2 and MS^3 was conducted on these putative metabolites. Based on our understanding of the metabolism of NNN and NNK[18] and tobacco alkaloids such as nicotine,[23] the 7 compounds in Table S7 were considered to specifically result from NNN metabolism. Targeted MS^2 and MS^3 analyses of all 7 compounds were performed in the U1* of the 3 rats. Their MS^2 and MS^3 fragmentation patterns are presented in Figure S6.

The targeted MS^2 analysis during this step differs from the one described above mainly due to the change of ion collisional dissociation mode. When HCD 30% for the targeted MS^2 analysis did not provide sufficient fragment ion information of the metabolites for proposing their structures, the collisional dissociation mode was switched to collision-induced dissociation (CID) at 30% that resulted in new MS^2 fragments in addition to previous results. The other MS parameters were: isolation mode, quadrupole; isolation window, *m/z* 1.5; activation time, 10 ms; detection type, Orbitrap; Orbitrap resolution, 60,000; scan range, *m/z* 100 – *m/z* 350; RF lens (%), 60; AGC target, standard; maximum injection time, 118 ms; microscans, 1; data type, profile; polarity, positive; use Easy-IC™, checked.

The targeted MS^3 analysis was conducted using the MS transitions listed in Table S7. The MS^2 precursor ions selected for the MS^3 fragmentation were based on their proposed structural specificity to the parent compound and their MS intensity. The MS parameters for the targeted MS^2 method are: MS isolation mode, quadrupole; MS isolation window, *m/z* 1.5; collision condition, HCD 30%; MS^2 isolation window, *m/z* 1.5; collision condition, HCD 35%; detection type, Orbitrap; Orbitrap resolution, 60,000; mass range, normal; scan range mode, auto; RF lens (%), 60; AGC target, standard; maximum injection time, 118 ms; microscans, 1; data type, profile; polarity, positive; use Easy-IC™, checked.

Confirmation of NNN metabolites by spiking experiments:

To verify the 6 known NNN metabolites observed in the urine, we performed spiking experiments by using their stable isotope-labeled internal standards. Two representative metabolites considered to specifically result from NNN metabolism were confirmed by spiking with their newly synthesized unlabeled standards.

To verify the known NNN metabolites, the d_0-U1 of the 3 rats treated with unlabeled NNN were used. The d_0-U1 (0.1 mL) was diluted into 0.9 mL PBS buffer (pH = 7) and then spiked with the isotope-labeled internal standards of [CH_2-d_4]HPB (500 pg),

[$^{13}C_6$]NNN (500 pg), [pyridine-d_4]NNN-*N*-oxide (2.5 pmol), [pyridine-d_4]keto acid (500 pg), [$^{13}C_6$]hydroxy acid (500 pg), and [pyridine-d_4]norcotinine (500 pg). The resulting mixture was processed using the same protocol as described above. However, due to the very low MS response (probably because of the strong ion suppression of the urine matrix), an additional amount of [CH_2-d_4]HPB (500 pg), [$^{13}C_6$]NNN (500 pg), and [pyridine-d_4]norcotinine (62.5 pg) was spiked into the sample. Since keto acid **18** and hydroxy acid **19** did not retain well on the cartridges, 500 pg of each of the corresponding internal standards was also spiked into the samples for the targeted MS analysis. The mass list included *m/z* 163.0866 (norcotinine), 166.0863 (HPB), 167.1117 ([pyridine-d_4]norcotinine), 170.1114 ([CH_2-d_4]HPB), 178.0975 (NNN), 180.0655 (keto acid), 182.0812 (hydroxy acid), 184.0906 ([pyridine-d_4]keto acid), 184.1176 ([$^{13}C_6$]NNN), 188.1013 ([$^{13}C_6$]hydroxy acid), 194.0924 (NNN-*N*-oxide), and 198.1175 ([pyridine-d_4]NNN-*N*-oxide).

To verify the newly identified NNN metabolites, the U1* from each of the 3 rats treated with NNN and [pyridine-d_4]NNN (0.1 mL each, in a 1:1 ratio) was diluted in 0.8 mL PBS buffer (pH = 7). The mixture was processed in the same way as described above. Five hundred pmol of the newly synthesized compounds **23** (MPBA) and **24** (Py-Pyrrole-Cys-NHAc) were spiked into the processed urine samples for the targeted MS analysis. The mass list included *m/z* 212.0740 and 216.0991 (**23** and [pyridine-d_4]**23**, respectively) and 306.0907 and 310.1158 (**24** and [pyridine-d_4]**24**, respectively).

RESULTS AND DISCUSSION

Metabolic profiling of NNN metabolites in the urine of laboratory animals has been previously accomplished using a radioflow HPLC method.[19,22] The principal metabolites identified from these studies can also be formed by the metabolism of NNK and nicotine. To investigate the urinary metabolites of NNN that specifically result from its metabolism, we adopted the high resolution mass spectrometry-based metabolic profiling method we previously developed[25] and improved the data analysis workflow to provide a more comprehensive metabolic profile of NNN in rat urine.

Rat study of NNN metabolism and urine sample purification

F344 rats have been previously used to analyze urinary metabolites of NNN[19] and were thus chosen for our current study gavaging 10 mg/kg NNN or [pyridine-d_4]NNN in H_2O. To minimize inter-individual differences in NNN metabolism, the compounds were administered to the same rats after a washout period of 4 days (Figure S3) since approximately 90% of NNN metabolites is excreted within 3 days after smoking cessation.[31] No obvious toxic effects were observed during the course of this study (Table S1).

The urine samples were collected and purified using the protocol reported before[25] but with the modification of adding β-glucuronidase prior to the sample purification steps. Considering that glucuronidation can readily occur to the pyridine ring of NNN as suggested by a high percentage (59.1 ± 26.0 and 61.8 ± 7.7%, respectively) of NNN-*N*-Gluc in total performed NNN in the urine of cigarette smokers and smokeless tobacco users,[32] it is likely that some NNN metabolites would be conjugated as glucuronides to some different extents. Since our goal was to identify new metabolites that are specifically formed from NNN, it

was beneficial to potentially increase the concentration of unconjugated NNN metabolites by pre-treating the urine with β-glucuronidase. The combinations of SPE cartridges and eluting conditions have also been examined and provide >50% recoveries of most of the known NNN metabolites.[25]

Untargeted and targeted MS^2 screening of rat urine

After SPE purification, the mixed urine samples and the PBS controls were analyzed by the untargeted MS screening method[25] with a major change of using a smaller scan range (*m/z* 100–500) to increase the assay sensitivity. The peak features were extracted with Compound Discoverer 3.2 and filtered using the updated version of the automated custom script (supplementary file) with the parameters described in Table 1. After removing all the redundant peaks (potential isomers, background peaks, contamination peaks, etc), the numbers of matched d_0–d_4 peak pairs identified in the urine of rats #1, 2 and 3 were 285, 228 and 206, respectively. As shown in Figure 2, there were 161 and 31 matched pairs detected in the U1* and U2* of at least 2 rats, respectively.

All 161 and 31 matched d_0–d_4 pairs identified in the U1* and U2* were re-analyzed by the targeted MS^2 screening method (Tables S3 and S4) to ensure their peak feature fidelity. The peak shapes, retention times and peak area ratios were manually examined to exclude any peak pairs with an anomalous pattern. The most common type of interfering peaks were the in-source-decay ions generated by the relatively abundant compounds such as NNN and NNN-*N*-oxide (Tables S5 and S6). The formation of dimers and clusters were also noted, for example, the dimer of NNN-*N*-oxide (Table S5, entry 150) and the cluster of 4-hydroxy-1-(pyridine-3-yl)butan-1-one (**15**, HPB) and [pyridine-d_4]HPB (Table S5, entry 132). The same types of interfering peaks were also observed in our previous study of NNK, suggesting relatively high concentrations of these metabolites being present in the urine.[25] MS^2 features of the d_0–d_4 peaks that passed the manual evaluation were scrutinized for their fragmentation patterns. Only matched pairs with a similar d_0–d_4 fragmentation pattern and at least 2–3 matched fragment ions (with a mass difference of 4.0251 ± 0.001 Da) were included for detailed structural analysis. This led to the generation of a list of 46 putative NNN metabolites as summarized in Table 2.

Putative NNN metabolites with proposed structural information

Based on the MS^2 fragmentation patterns, structures of the majority of the 46 putative metabolites (Table 2) were proposed using the same logic reported before.[25] For example, the best formula corresponding to *m/z* 212.0740 is $C_{10}H_{14}NO_2S^+$ with 0 ppm mass difference (Figure S5, # 23). The abundant MS^2 ions of *m/z* 164.0705, 148.0757 and 106.0650 strongly suggested the parental compound having a high structural similarity to the known NNN metabolite hydroxy acid **19**. The presence of a unique feature of *m/z* 124.0217 (with the best-predicted formula of $C_6H_6NS^+$ with 1.6 ppm mass difference) provided convincing evidence that a methylthiol group was attached to the adjacent carbon of the pyridine ring (carbinol methylthiol). Considering that NNN undergoes 5′-hydroxylation to generate reactive intermediates[33–37] that may react with thiol-containing sources, we deduced that the most likely structure of *m/z* 212.0740 was compound **25** (Figure 1). Using the strategy described above, we were able to propose 32 most likely structures out of the

total of 46 putative metabolites as summarized in Table 2. The proposed structures and the MS^2 fragmentation patterns of the metabolites are presented in Figures S4 and S5.

Based on the proposed structures, 5 groups of metabolites are summarized in Table 2. The known NNN metabolites (most of them being verified as presented below) and their putative methylation products agreed with most of the known NNN metabolites. The derivatives resulting from oxidation, denitrosation, and solvolysis of known NNN metabolites were also considered to be reasonable based on our knowledge of NNN metabolism.. To our surprise, a relatively large number of potential thiol-containing metabolites formed from NNN were identified, as shown in the Table 2. Even though the endogenous pathways to form these thiol-containing compounds are still largely unknown, we hypothesize that glutathione conjugation may play an important role here due to the observation of a few putative cysteine adducts (e.g., **22**, **24**, Figure 1) that typically result from glutathione biotransformation reactions. Considering that some of these putative metabolites likely result from NNN metabolic activation pathways – 2′- and 5′-hydroxylation – synthesis of the two representative compounds **23** and **24** was pursued for peak identification.

Structural confirmation of known metabolites resulted from NNN metabolism

The major metabolites identified in the urine of rats treated with NNN include hydroxy acid **19**, keto acid **18**, NNN-*N*-oxide (**6**), and norcotinine (**8**), together with unmodified NNN (**1**).[19] The other compounds such as HPB (**15**) were also identified in previous studies as minor urinary metabolites.[19–21] All these known metabolites were successfully identified in the rat urine using our metabolic profiling method, suggesting its great potential of comprehensively analyzing complex samples in a urine matrix. Even though the MS^2 evidence for the known metabolites was convincing (Figure S5), confirmation of the structures by comparison to their synthetic standards was required. As shown in Figure 3, the formation of NNN, NNN-*N*-oxide, norcotinine, HPB and keto acid was clearly confirmed by their co-elution with the corresponding isotopically labeled internal standards. The peak for hydroxy acid was also observed but with poor column retention under the conditions used here (data not shown).[28]

In addition, the formation of other minor metabolites such as 1,4-diol **14** and 1,3-diol **21** were also confirmed by comparing to the reported data from our NNK metabolism study.[25] As shown in Figures 4 and S5 #3, the fragmentation patterns of the 1,4-diol peak at 14.9 min and the 1,3-diol peak at 15.9 min agreed with that of the NNK study in which 1,4-diol and 1,3-diol were confirmed by comparison to the synthetic standards. We also observed the formation of one unknown diol isomer at 16.6 min, presenting a fragmentation pattern consistent with that of the other 2 known peaks. This unknown isomer peak was also observed in the NNK study.[25]

Similarly, the formation of the metabolites *N*-acetyl-*S*-(4-hydroxy-4-(pyridin-3-yl)butyl)-L-cysteine (PHB-Cys-NHAc, **22**) and its isomers (structures shown in Figure S5, #40) were confirmed by comparing them to the MS data obtained in the NNK study.[25] As shown in Figure 5, the MS^2 fragmentation pattern of the peak at 17.9 min features two predominant ions at *m/z* 148.0425 and 132.0806, both of which are characteristic for the structural assignment. The ion at *m/z* 148.0425 corresponds to the structure of *N*-acetyl cysteine

with the loss of oxygen; the ion at *m/z* 132.0806 has been consistently observed in NNN-derived compounds (e.g. pyridylhydroxybutyl (PHB)-DNA adducts[38–40]) and corresponds to the structure of PHB with the loss of H_2O and H_2. The existence of the ion with *m/z* 190.0531 further suggested the metabolite structure containing *N*-acetyl cysteine. The same MS^2 fragmentation pattern and isomer peak profiles were observed in the NNK study.[25] Considering that the same reactive intermediate can be formed by both NNK α-methyl hydroxylation and NNN 2′-hydroxylation,[18] the formation of PHB-Cys-NHAc and its isomers in this NNN-treated rat urine was not a surprise. They are likely to be detoxification products resulting from the reaction with glutathione followed by a cascade of enzymatic hydrolysis and *N*-acetylation transformations.[41]

Synthesis and structural confirmation of new metabolites specifically formed by NNN

Among the 46 putative metabolites of NNN, we were most interested in metabolites that are specifically formed from NNN, since they may serve as potential biomarkers for monitoring NNN exposure and uptake in tobacco users. On the basis of our understanding of the metabolism of NNN and its closely associated compounds NNK[18] and nicotine,[23] we speculated that there were 7 putative metabolites formed exclusively from NNN (Table S7). Targeted MS^2 and MS^3 analyses of the 7 compounds were conducted with the U1* of all 3 rats. The MS data and their proposed MS fragment ion structures are presented in Figure S6.

Based on their structural similarity, these 7 compounds can be classified into 3 groups (Table S7): the NNN derivatives (**S6** and **S8**), the pyridine-pyrrole derivatives (**S11** and **24**), and the carbinol thiol compounds (**23**, **S13** and **S16**). To verify the proposed structures of **23** and **24**, we synthesized the standards using the method shown in Scheme 2. Starting from **25** that can be synthesized as previously reported,[29] the intermediate **26** was obtained by $NaBH_4$ reduction. It was then converted to the methylthio intermediate **28** either by a direct conversion with dimethyl disulfide or via the sulfonate intermediate **27**. The desired product **23** was obtained after the hydrolysis of **28** in the presence of LiOH. To synthesize **24**, iodination of β-nornicotyrine (**29**) with *N*-iodosuccinimide yielded the intermediate **30** along with 2 major side products 4′-iodo-β-nornicotyrine and 4′, 5′-diiodo-β-nornicotyrine. Compound **30** reacted with *N*-acetyl-L-cysteine (**31**) and generated the desired product **24** in a low yield. Both compounds were fully characterized by NMR and HRMS. Their NMR spectra are presented in Figures S1 and S2; their MS^2 fragmentation patterns are presented in Figure 6.

Using the synthesized standards, we confirmed the formation of metabolites **23** and **24** in the U1* urines of all 3 rats. As shown in Figures 6 and S7, the peaks corresponding to **23** and **24** are augmented by spiking the synthesized standards into the urine. The major MS^2 fragment ions of the peaks in the urine are also in agreement with the ones observed from the standards. We hypothesized that the formation of **23** and **24** resulted from the NNN 5′-hydroxylation pathway – one of the major metabolic activation pathways – by reaction with endogenous thiols such as glutathione followed by sequential biotransformation (Scheme S1). However, the exclusive formation of these 2 metabolites from NNN metabolism (as opposed to nicotine or NNK) requires further study. The targeted MS analysis of **23** and **24** in the urine of tobacco users is currently in progress.

CONCLUSIONS

In summary, for the first time we characterized 2 new metabolites **23** and **24** that may specifically result from NNN metabolism by using a modified high-resolution mass spectrometry-based stable-isotope labeling method. Their structures were confirmed by comparing them to fully characterized synthesized standards. The formation of these urinary metabolites with potential specificity to NNN metabolism holds promise for their use as putative biomarkers to monitor the uptake and metabolism of this important tobacco carcinogen in cigarette smokers and smokeless tobacco users.

Supplementary Material

Refer to Web version on PubMed Central for supplementary material.

ACKNOWLEDGMENTS

The authors thank Dr. Lisa Peterson and Karin Vevang for providing the metabolism cages, and Dr. Lakmal Rozumalski for gavaging the rats. We thank Drs. Peter Villalta and Yingchun Zhao for help with the operation of the mass spectrometer. The help of upgrading the custom JAVA script from Dr. Jie Li (Department of Computer Science and Engineering, University of Minnesota) and suggestions for the synthesis of compound **23** (MPBA) from Prof. Tianfeng Xu (Shanghai Institute of Materia Medica, Chinese Academy of Sciences) are greatly appreciated by Y.L. We are grateful for the editorial assistance provided by Robert (Bob) Carlson.

Funding

This study was supported by grant CA-81301 from the National Cancer Institute. Mass spectrometry was carried out in the Analytical Biochemistry Shared Resource of the Masonic Cancer Center, University of Minnesota, supported in part by Cancer Center Support Grant CA-077598.

ABBREVIATIONS

BU	baseline urine
DCM	dichloromethane
1,4-diol	1-(pyridin-3-yl)butane-1,4-diol
HPB	4-hydroxy-1-(pyridine-3-yl)butan-1-one
HPLC	high performance liquid chromatography
HRMS	high-resolution mass spectrometry
MPBA	4-(methylthio)-4-(pyridin-3-yl)butanoic acid
NNC	*N*′-Nitrosonorcotinine
NNK	4-(*N*-nitrosomethylamino)-1-(3-pyridyl)-1-butanone
NNN	*N*′-nitrosonornicotine
NNN-*N*-Gluc	*N*-glucuronide of NNN
NNN-*N*-oxide	*N*′-nitrosonornicotine-1*N*-oxide

PHB	pyridylhydroxybutyl
PHB-Cys-NHAc	*N*-acetyl-*S*-(4-hydroxy-4-(pyridin-3-yl)butyl)-L-cysteine
Py-Pyrrole-Cys-NHAc	*N*-acetyl-*S*-(5-(pyridin-3-yl)-1*H*-pyrrol-2-yl)-L-cysteine

REFERENCES

1. Hoffmann D; Hecht SS; Ornaf RM; Wynder EL *N*'-nitrosonornicotine in tobacco. Science 1974, 186, 265–267. [PubMed: 4414773]
2. Klus H; Kuhn H Determination of nornicotine nitrosamine in the smoke condensate of nornicotine-rich cigarettes. Fachl. Mitt. Oesterreichischen 1973, 14, 251–257.
3. Li Y; Hecht SS Carcinogenic components of tobacco and tobacco smoke: A 2022 update. Food Chem. Toxicol. 2022, 165, 113179. [PubMed: 35643228]
4. Edwards SH; Rossiter LM; Taylor KM; Holman MR; Zhang L; Ding YS; Watson CH Tobacco-specific nitrosamines in the tobacco and mainstream smoke of U.S. commercial cigarettes. Chem. Res. Toxicol. 2017, 30, 540–551. [PubMed: 28001416]
5. Edwards SH; Hassink MD; Taylor KM; Watson CH; Kuklenyik P; Kimbrell B; Wang L; Chen P; Valentín-Blasini L Tobacco-specific nitrosamines in the tobacco and mainstream smoke of commercial little cigars. Chem. Res. Toxicol. 2021, 34, 1034–1045. [PubMed: 33667338]
6. Hecht SS; Hatsukami DK Smokeless tobacco and cigarette smoking: Chemical mechanisms and cancer prevention. Nat. Rev. Cancer 2022, 22, 143–155. [PubMed: 34980891]
7. Nasrin S; Chen G; Watson CJW; Lazarus P Comparison of tobacco-specific nitrosamine levels in smokeless tobacco products: High levels in products from Bangladesh. PLoS One 2020, 15, e0233111. [PubMed: 32453764]
8. U.S. Food and Drug Administration. Tobacco product standard for *N*-nitrosonornicotine level in finished smokeless tobacco products. Fed. Regist. 2017, 82, 8004–8053.
9. Hecht SS Biochemistry, biology, and carcinogenicity of tobacco-specific *N*-nitrosamines. Chem. Res. Toxicol. 1998, 11, 559–603. [PubMed: 9625726]
10. Sinha DN; Abdulkader RS; Gupta PC Smokeless tobacco-associated cancers: A systematic review and meta-analysis of Indian studies. Int. J. Cancer 2016, 138, 1368–1379. [PubMed: 26443187]
11. Critchley JA; Unal B Health effects associated with smokeless tobacco: a systematic review. Thorax 2003, 58, 435–443. [PubMed: 12728167]
12. Boffetta P; Hecht S; Gray N; Gupta P; Straif K Smokeless tobacco and cancer. Lancet Oncol. 2008, 9, 667–675. [PubMed: 18598931]
13. Khan Z; Tönnies J; Müller S Smokeless tobacco and oral cancer in South Asia: A systematic review with meta-analysis. J. Cancer Epidemiol. 2014, 2014, 394696. [PubMed: 25097551]
14. Gupta AK; Kanaan M; Siddiqi K; Sinha DN; Mehrotra R Oral cancer risk assessment for different types of smokeless tobacco products sold worldwide: A review of reviews and meta-analyses. Cancer. Prev. Res. 2022, 15, 733–746.
15. International Agency for Research on Cancer. Personal Habits and Indoor Combustions, IARC Monographs on the Evaluation of Carcinogenic Risks to Humans; IARC: Lyon, FR, 2012; Vol. 100E.
16. Yuan JM; Knezevich AD; Wang R; Gao YT; Hecht SS; Stepanov I Urinary levels of the tobacco-specific carcinogen *N*'-nitrosonornicotine and its glucuronide are strongly associated with esophageal cancer risk in smokers. Carcinogenesis 2011, 32, 1366–1371. [PubMed: 21734256]
17. Yang J; Carmella SG; Hecht SS Analysis of *N*'-nitrosonornicotine enantiomers in human urine by chiral stationary phase liquid chromatography-nanoelectrospray ionization-high resolution tandem mass spectrometry. J. Chromatogr. B 2017, 1044–1045, 127–131.
18. Li Y; Hecht SS Metabolism and DNA adduct formation of tobacco-specific *N*-nitrosamines. Int. J. Mol. Sci. 2022, 23, 5109. [PubMed: 35563500]
19. Hecht SS; Lin D; Chen CB Comprehensive analysis of urinary metabolites of *N*'-nitrosonornicotine. Carcinogenesis 1981, 2, 833–838. [PubMed: 7296768]

20. Hecht SS; Young R Regiospecificity in the metabolism of the homologous cyclic nitrosamines, N'-nitrosonornicotine and *N'*-nitrosoanabasine. Carcinogenesis 1982, 3, 1195–1199. [PubMed: 7172419]
21. Hoffmann D; Castonguay A; Rivenson A; Hecht SS Comparative carcinogenicity and metabolism of 4-(methylnitrosamino)-1-(3-pyridyl)-1-butanone and *N'*-nitrosonornicotine in Syrian golden hamsters. Cancer Res. 1981, 41, 2386–2393. [PubMed: 7237437]
22. Upadhyaya P; Zimmerman CL; Hecht SS Metabolism and pharmacokinetics of *N'*-nitrosonornicotine in the patas monkey. Drug Metab. Dispos. 2002, 30, 1115–1122. [PubMed: 12228188]
23. Murphy SE Biochemistry of nicotine metabolism and its relevance to lung cancer. J. Biol. Chem. 2021, 296, 100722. [PubMed: 33932402]
24. Li Y; Hecht SS Mass spectrometric quantitation of *N'*-nitrosonornicotine-1*N*-oxide in the urine of cigarette smokers and smokeless tobacco users. Chem. Res. Toxicol. 2022, 35, 1579–1588. [PubMed: 36006857]
25. Dator R; von Weymarn LB; Villalta PW; Hooyman CJ; Maertens LA; Upadhyaya P; Murphy SE; Balbo S *In vivo* stable-isotope labeling and mass-spectrometry-based metabolic profiling of a potent tobacco-specific carcinogen in rats. Anal Chem 2018, 90, 11863–11872. [PubMed: 30086646]
26. Balbo S; James-Yi S; Johnson CS; O'Sullivan MG; Stepanov I; Wang M; Bandyopadhyay D; Kassie F; Carmella S; Upadhyaya P; Hecht SS (*S*)-*N'*-Nitrosonornicotine, a constituent of smokeless tobacco, is a powerful oral cavity carcinogen in rats. Carcinogenesis 2013, 34, 2178–2183. [PubMed: 23671129]
27. Stepanov I; Muzic J; Le CT; Sebero E; Villalta P; Ma B; Jensen J; Hatsukami D; Hecht SS Analysis of 4-hydroxy-1-(3-pyridyl)-1-butanone (HPB)-releasing DNA adducts in human exfoliated oral mucosa cells by liquid chromatography-electrospray ionization-tandem mass spectrometry. Chem. Res. Toxicol. 2013, 26, 37–45. [PubMed: 23252610]
28. Jing M; Wang Y; Upadhyaya P; Jain V; Yuan JM; Hatsukami DK; Hecht SS; Stepanov I Liquid chromatography-electrospray ionization-tandem mass spectrometry quantitation of urinary [pyridine-D4]4-hydroxy-4-(3-pyridyl)butanoic acid, a biomarker of 4-(methylnitrosamino)-1-(3-pyridyl)-1-butanone metabolic activation in smokers. Chem. Res. Toxicol. 2014, 27, 1547–1555. [PubMed: 25098652]
29. Carlson ES; Upadhyaya P; Hecht SS Evaluation of nitrosamide formation in the cytochrome p450-mediated metabolism of tobacco-specific nitrosamines. Chem. Res. Toxicol. 2016, 29, 2194–2205. [PubMed: 27989137]
30. Vega Iel D; Gale PA; Light ME; Loeb SJ NH vs. CH hydrogen bond formation in metal-organic anion receptors containing pyrrolylpyridine ligands. Chem. Commun. 2005, 4913–4915.
31. Stepanov I; Carmella SG; Briggs A; Hertsgaard L; Lindgren B; Hatsukami D; Hecht SS Presence of the carcinogen *N'*-nitrosonornicotine in the urine of some users of oral nicotine replacement therapy products. Cancer Res. 2009, 69, 8236–8240. [PubMed: 19843845]
32. Stepanov I; Hecht SS Tobacco-specific nitrosamines and their pyridine-*N*-glucuronides in the urine of smokers and smokeless tobacco users. Cancer Epidemiol. Biomarkers Prev. 2005, 14, 885–891. [PubMed: 15824160]
33. Zarth AT; Upadhyaya P; Yang J; Hecht SS DNA adduct formation from metabolic 5'-hydroxylation of the tobacco-specific carcinogen *N'*-nitrosonornicotine in human enzyme systems and in rats. Chem. Res. Toxicol. 2016, 29, 380–389. [PubMed: 26808005]
34. Li Y; Carlson ES; Zarth AT; Upadhyaya P; Hecht SS Investigation of 2'-deoxyadenosine-derived adducts specifically formed in rat liver and lung DNA by *N'*-nitrosonornicotine metabolism. Chem. Res. Toxicol. 2021, 34, 1004–1015. [PubMed: 33720703]
35. Li Y; Hecht SS Identification of an *N'*-nitrosonornicotine-specific deoxyadenosine adduct in rat liver and lung DNA. Chem. Res. Toxicol. 2021, 34, 992–1003. [PubMed: 33705110]
36. Upadhyaya P; Hecht SS Identification of adducts formed in the reactions of 5'-acetoxy-*N'*-nitrosonornicotine with deoxyadenosine, thymidine, and DNA. Chem. Res. Toxicol. 2008, 21, 2164–2171. [PubMed: 18821782]

37. Upadhyaya P; McIntee EJ; Villalta PW; Hecht SS Identification of adducts formed in the reaction of 5'-acetoxy-*N'*-nitrosonornicotine with deoxyguanosine and DNA. Chem. Res. Toxicol. 2006, 19, 426–435. [PubMed: 16544948]

38. Li Y; Ma B; Cao Q; Balbo S; Zhao L; Upadhyaya P; Hecht SS Mass spectrometric quantitation of pyridyloxobutyl DNA phosphate adducts in rats chronically treated with *N'*-nitrosonornicotine. Chem. Res. Toxicol. 2019, 32, 773–783. [PubMed: 30740971]

39. Ma B; Zarth AT; Carlson ES; Villalta PW; Stepanov I; Hecht SS Pyridylhydroxybutyl and pyridyloxobutyl DNA phosphate adduct formation in rats treated chronically with enantiomers of the tobacco-specific nitrosamine metabolite 4-(methylnitrosamino)-1-(3-pyridyl)-1-butanol. Mutagenesis 2017, 32, 561–570. [PubMed: 29186507]

40. Carlson ES; Upadhyaya P; Villalta PW; Ma B; Hecht SS Analysis and identification of 2'-deoxyadenosine-derived adducts in lung and liver DNA of F-344 rats treated with the tobacco-specific carcinogen 4-(methylnitrosamino)-1-(3-pyridyl)-1-butanone and enantiomers of its metabolite 4-(methylnitrosamino)-1-(3-pyridyl)-1-butanol. Chem. Res. Toxicol. 2018, 31, 358–370. [PubMed: 29651838]

41. Hanna PE; Anders MW The mercapturic acid pathway. Crit. Rev. Toxicol. 2019, 49, 819–929. [PubMed: 31944156]

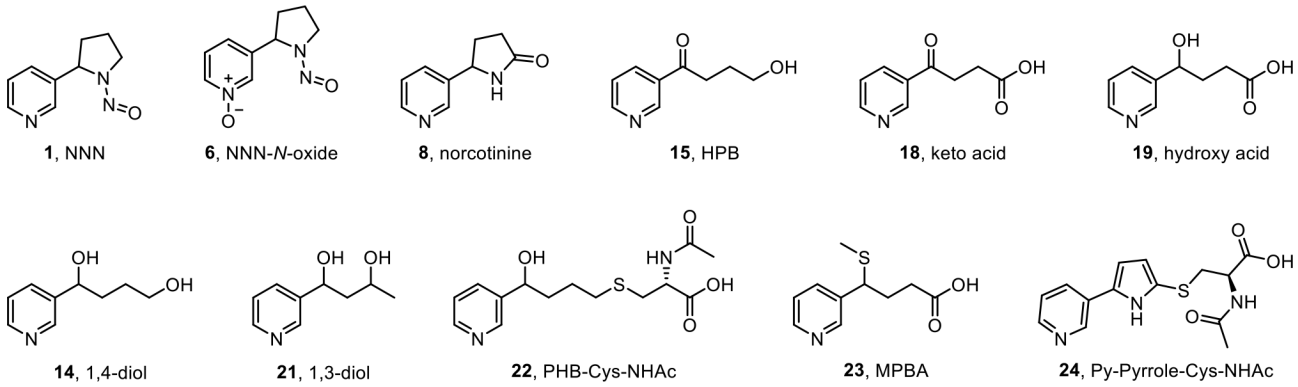

Figure 1.

Structures of known major NNN metabolites and compounds **14** and **21**-**24** identified in this study.

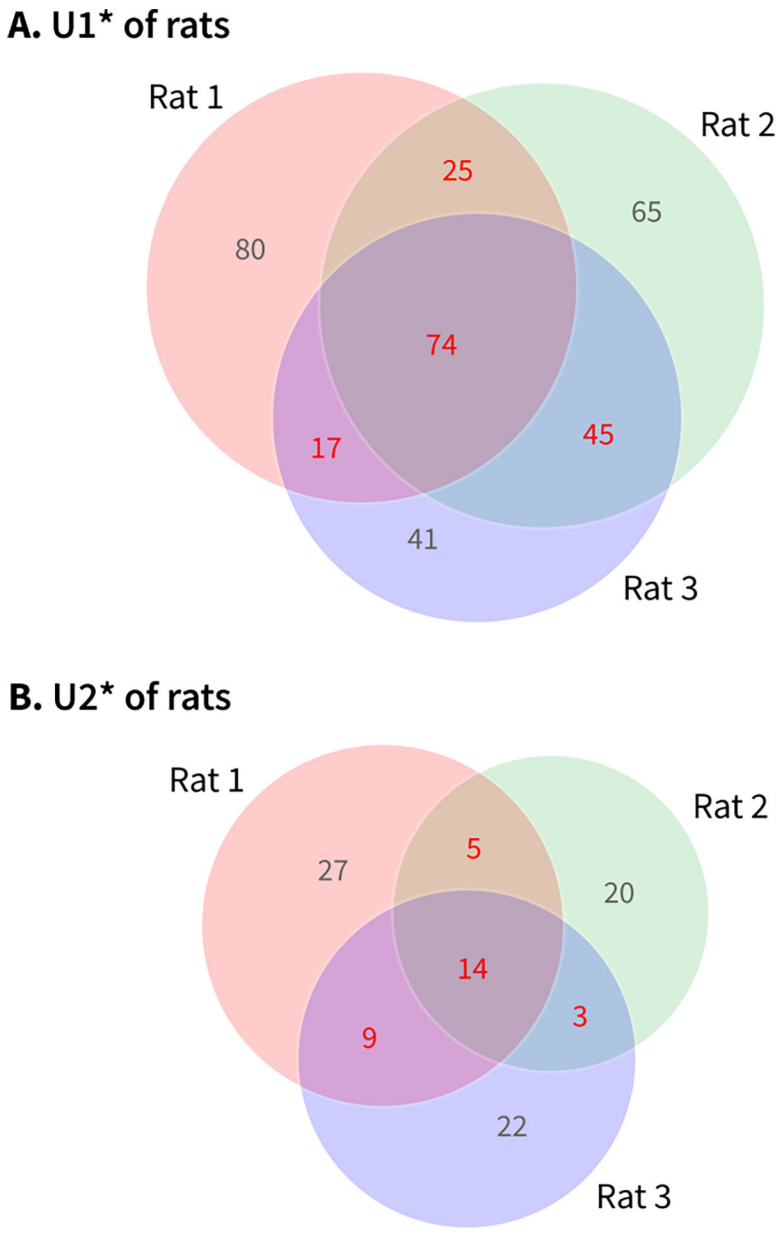

Figure 2.
Distribution patterns of matched d_0-d_4 peak pairs in the U1* (A) and U2* (B) urine of rats.

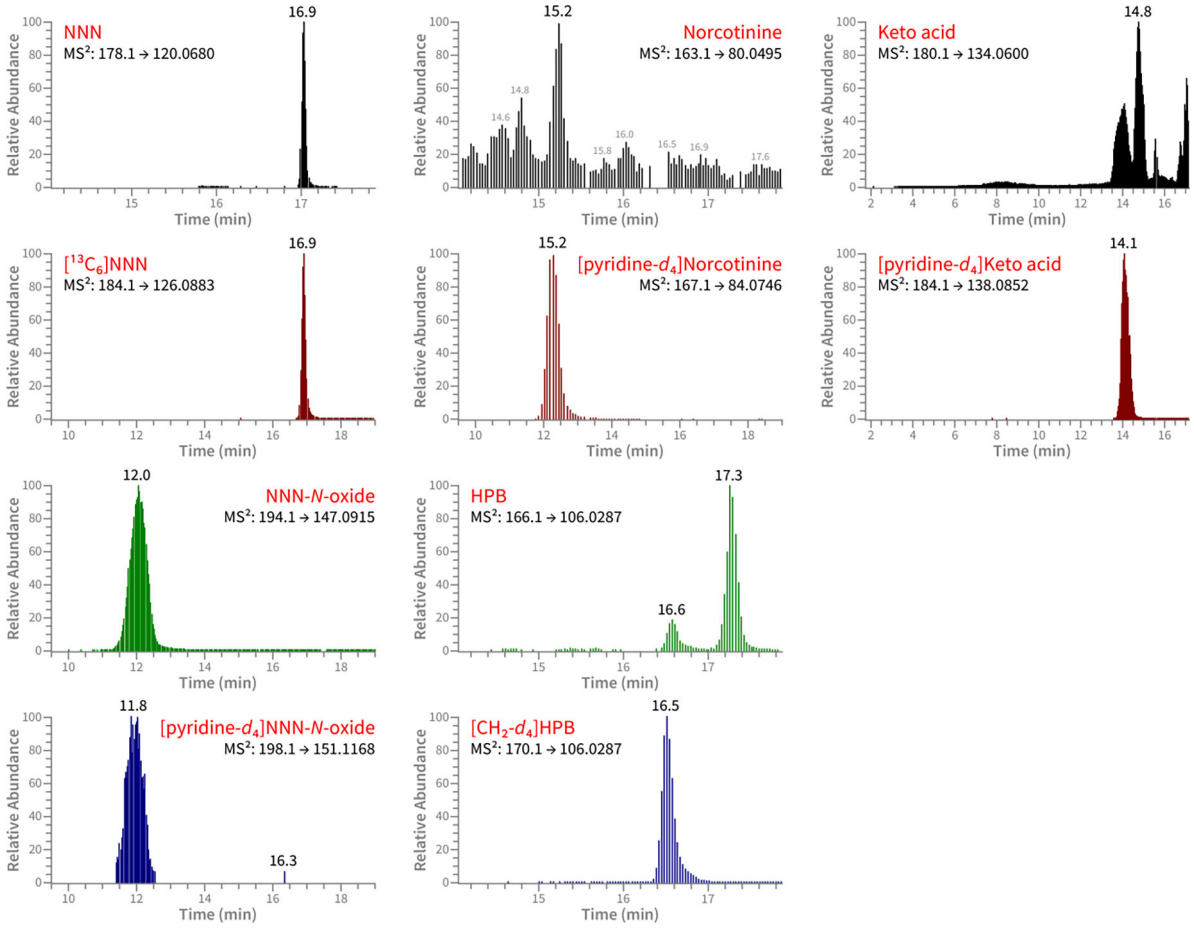

Figure 3.

NNN and four known major NNN metabolites that co-eluted with their corresponding isotopically labeled standards in the U1* of rat #3. The internal standards include [pyridine-d_4]keto acid, [pyridine-d_4]norcotinine, [$^{13}C_6$]NNN, [pyridine-d_4]NNN-*N*-oxide and [CH_2-d_4]HPB.

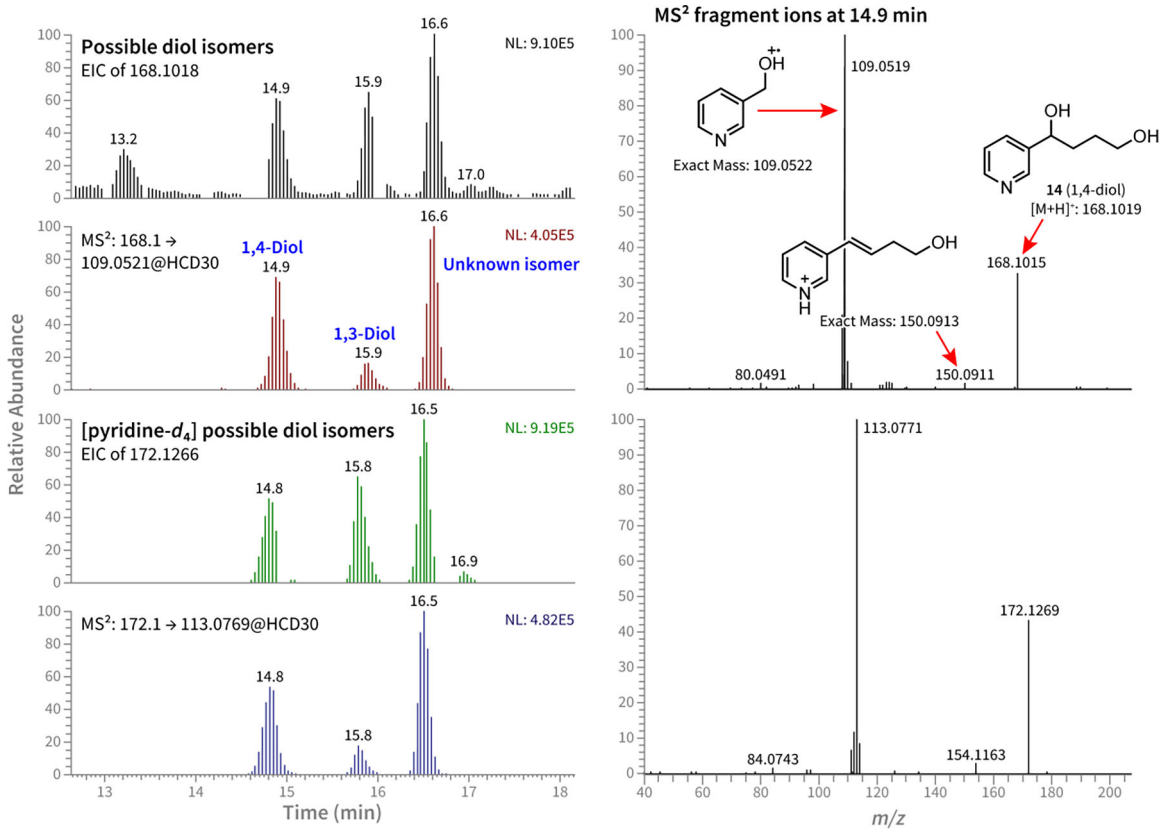

Figure 4.

LC traces of the diol isomers and the MS^2 fragmentation patterns of 1,4-diol **14** in the U2* of rat #1.

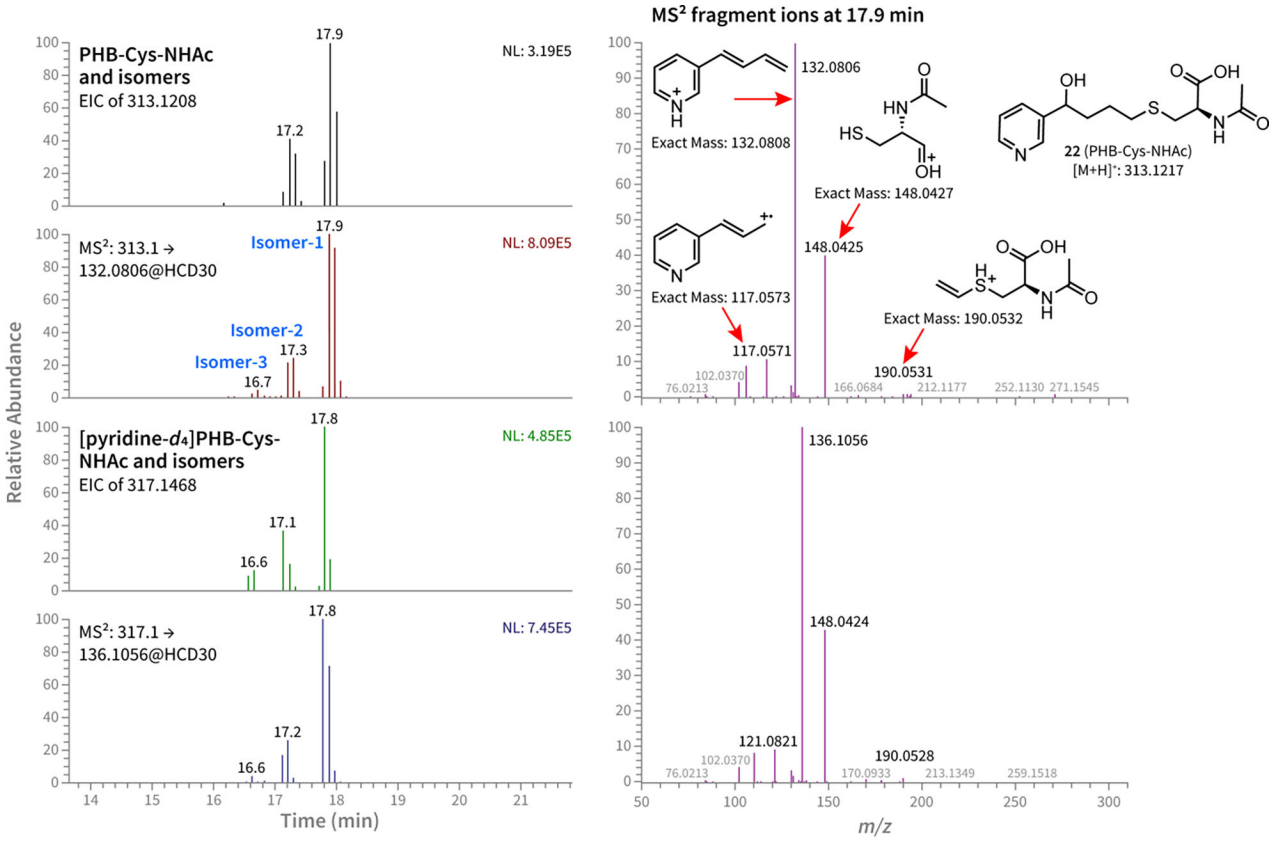

Figure 5.

LC traces and MS^2 fragmentation patterns of PHB-Cys-NHAc (**22**) and its isomers in the U1* of rat #1.

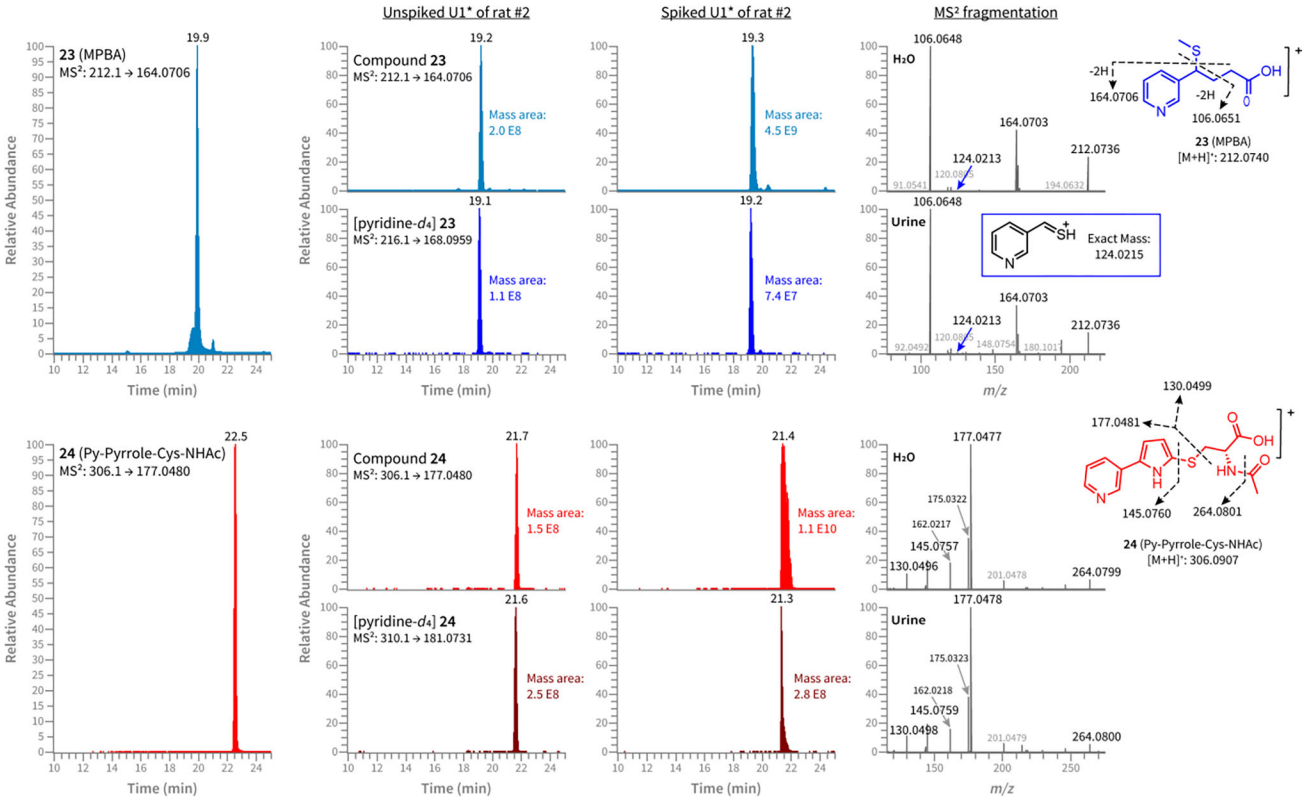

Figure 6.

The formation of new NNN metabolites **23** and **24** was confirmed by spiking their synthesized standards to the U1* of rat #2.

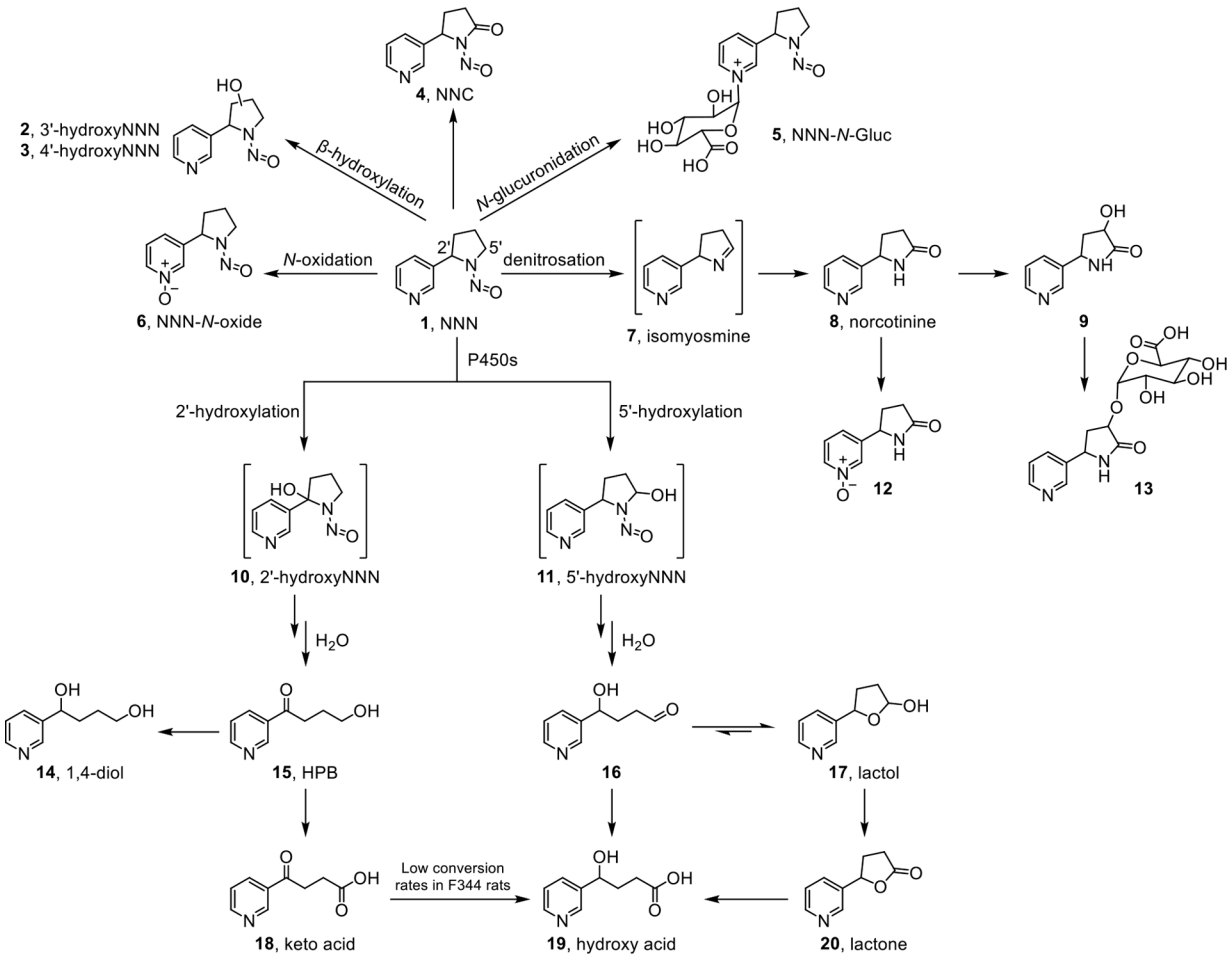

Scheme 1.

Established metabolism pathways of NNN and commonly used metabolite names.

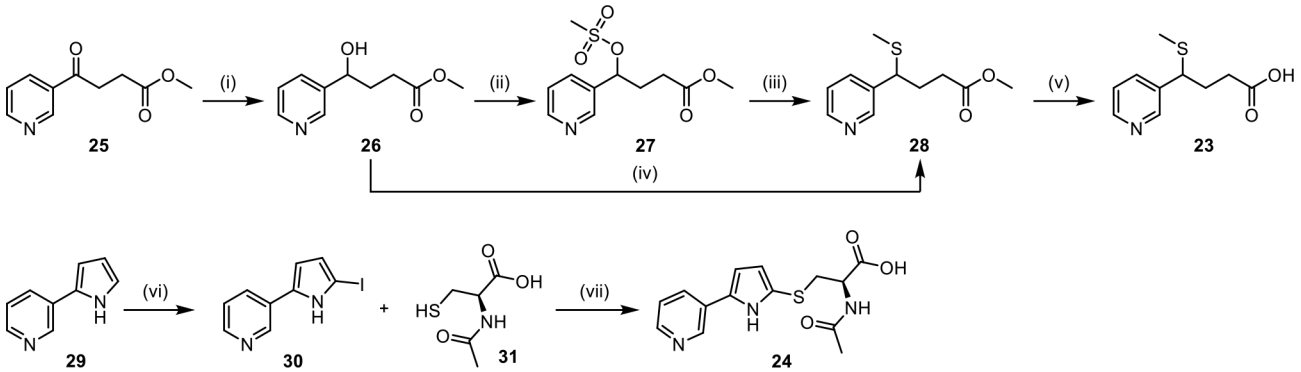

Scheme 2.

Synthesis of chemical standards **23** and **24**.

Reagents and conditions: (i) $NaBH_4$, THF, 0 °C to 25 °C, 2 h; (ii) methanesulfonyl chloride, Et_3N, DCM, 0 °C, 0.5 h; (iii) CH_3SNa, THF, 50 °C, 1.5 h; (iv) dimethyl disulfide, $P(Bu)_3$, THF, 25 °C, 2 h; (v) LiOH, THF/H_2O, 25 °C, overnight; 0.1 M HCl, pH = 6; (vi) *N*-iodosuccinimide, DMF, −10°C then 0 °C, 2 h; (vii) Et_3N, DMF, 90 °C, 3 h.

Table 1.

Numbers of matched d_0–d_4 peak pairs detected in the urine of F344 rats after administration of NNN or [pyridine-d_4]NNN.

	Rat #1				Rat #2				Rat #3			
	PBS	**BU***	**U1***	**U2***	**PBS**	**BU***	**U1***	**U2***	**PBS**	**BU***	**U1***	**U2***
Total peaks after CD feature extraction (peak area ≥ 500)	9875	15803	15858	15813	8449	12972	13672	13600	8215	12771	13458	13829
Matched peak pairs after automated peak picking (*m/z* 4.0251 ± 0.001)	1208	2941	4416	3129	987	1891	3533	2500	914	1855	3144	2481
Matched peak pairs after retention time filtering (Δ t_R: ± 0.2 min)	28	46	307	95	26	49	382	85	21	34	330	81
Matched peak pairs after peak area ratio filtering (ratio of 0.1 – 10)	15	28	274	71	14	30	343	70	8	23	298	64
Matched peak pairs after background peak removal and t_R filtering (t_R > 5 min)[a]	285				228				206			
Total matched d_0-d_4 peak pairs	397											

[a] Isomer peaks were counted only once.

Table 2.

Forty-six matched d_0–d_4 peak pairs identified in rat urine with proposed structural information.

No.	Rat #1		Rat #2		Rat #3		d_0_m/z	d_4_m/z	Description
	U1*	U2*	U1*	U2*	U1*	U2*			
Known NNN metabolites									
1	√	√	√	√	√	√	163.0864	167.1114	Norcotinine (**8**)
2	√				√		166.0862	170.1113	4-Hydroxy-1-(pyridine-3-yl)butan-1-one (**15**, HPB)
3		√		√			168.1018	172.1266	1-(Pyridin-3-yl)butane-1,4-diol (**14**, 1,4-Diol) and 1,3-diol (**21**) and the unknown diol
4	√	√	√	√	√	√	178.0975	182.1225	*N*-Nitrosonornicotine (**1**, NNN)
5	√		√	√			180.0654	184.0904	4-Oxo-4-(pyridin-3-yl)butanoic acid (**18**, Keto acid)
6	√		√	√	√		192.0768	196.1019	*N*-Nitrosonorcotinine (**4**, NNC)
7	√	√	√			√	194.0923	198.1175	*N*′-Nitrosonornicotine-1*N*-oxide (**6**, NNN-*N*-oxide)
Putative methylation products of known NNN metabolites									
8	√		√		√		177.1022	181.1273	Cotinine (**S1**)
9			√		√		180.1018	184.1269	3-(5-Methoxytetrahydrofuran-2-yl)pyridine (**S2**)
10	√		√		√		196.0968	200.1219	Methyl 4-hydroxy-4-(pyridin-3-yl)butanoate (**S3**)
11	√		√		√		208.1078	212.1330	4′-MethoxyNNN (**S4**)
12	√		√	√	√	√	210.1124	214.1376	Methyl 4-methoxy-4-(pyridin-3-yl)butanoate (**S5**)
Putative metabolites resulted from NNN oxidation, solvolysis, and/or denitrosation									
13	√		√				174.0658	178.0909	*N*-Nitrosonornicotyrine (**S6**)
14	√		√		√		175.0500	179.0752	3-(2-Oxo-2*H*-pyrrol-5-yl)pyridine 1-oxide (**S7**)
15	√		√		√		176.0818	180.1069	*N*-Nitrosoisomyosmine (**S8**)
16	√	√	√	√		√	178.0862	182.1112	Methyl (*E*)-4-(pyridin-3-yl)but-3-enoate (**S9**)
17	√		√		√		210.0872	214.1122	4′-HydroxyNNN-*N*-oxide (**S10**)
Putative thiol-containing metabolites									
18	√		√		√		207.0586	211.0838	3-(5-(Methylsulfinyl)-1*H*-pyrrol-2-yl)pyridine (**S11**)
19	√	√	√		√	√	212.0740	216.0990	4-(Methylthio)-4-(pyridin-3-yl)butanoic acid (**23**, MPBA)
20	√	√	√	√	√	√	214.0895	218.1147	Also shown in the NNK study [a]; 4-(Methylthio)-1-(pyridin-3-yl)butane-1,3-diol (**S12**)
21	√	√	√	√	√	√	226.0896	230.1147	Methyl 4-(methylthio)-4-(pyridin-3-yl)butanoate (**28**)
22		√		√		√	228.0511	232.0762	*S*-Methyl 4-mercapto-4-(pyridin-3-yl)butanethioate (**S13**)
23	√		√		√		228.0688	232.0934	4-Hydroxy-4-(methylsulfinyl)-1-(pyridin-3-yl)butan-1-one (**S14**)
24	√	√	√		√		230.0844	234.1096	4-(Methylsulfinyl)-1-(pyridin-3-yl)butane-1,3-diol (**S15**)
25	√	√	√		√		242.0846	246.1096	Methyl 3-hydroxy-4-(methylthio)-4-(pyridin-3-yl)butanoate (**S16**)
26	√		√		√		295.1111	299.1362	(*E*)-*N*-Acetyl-*S*-(4-(pyridin-3-yl)but-3-en-1-yl)-L-cysteine (**S17**)
27	√		√	√	√		299.1059	303.1310	Methyl *S*-(2-hydroxy-4-oxo-4-(pyridin-3-yl)butyl)-L-cysteinate (**S18**) or 4-(((*R*)-2-Amino-3-methoxy-3-oxopropyl)thio)-4-(pyridin-3-yl)butanoic acid (**S19**)

No.	Rat #1		Rat #2		Rat #3		d_0_m/z	d_4_m/z	Description
	U1*	U2*	U1*	U2*	U1*	U2*			
28	√	√	√		√		306.0907	310.1158	*N*-Acetyl-*S*-(5-(pyridin-3-yl)-1*H*-pyrrol-2-yl)cysteine (**24**, Py-Pyrrole-Cys-NHAc)
29	√		√		√	√	311.1060	315.1311	*N*-Acetyl-*S*-(4-oxo-4-(pyridin-3-yl)butyl)-L-cysteine (**S20**, POB-Cys-NHAc) or *N*-acetyl-S-(5-(pyridin-3-yl)tetrahydrofuran-2-yl)-L-cysteine (**S21**, Py-THF-Cys-NHAc)
30	√	√	√	√	√	√	313.1208	317.1468	*N*-Acetyl-S-(4-hydroxy-4-(pyridin-3-yl)butyl)-L-cysteine (**22**, PHB-Cys-NHAc) or its isomers
31	√		√		√		320.1063	324.1314	Methyl *N*-acetyl-*S*-(5-(pyridin-3-yl)-1*H*-pyrrol-2-yl)cysteinate (**S22**, Py-Pyrrole-Cys-NHAc methyl ester)
32	√	√	√	√	√		327.1373	331.1624	Methyl *N*-acetyl-*S*-(4-hydroxy-4-(pyridin-3-yl)butyl)-L-cysteinate (**S23**, PHB-Cys-NHAc methyl ester)
Putative metabolites with limited structural information									
33	√		√		√		191.1179	195.1430	
34			√		√		195.0958	199.1208	
35	√				√		198.0582	202.0833	
36	√		√		√		207.0764	211.1015	
37	√		√	√	√	√	212.1030	216.1280	
38			√		√		220.0968	224.1220	
39	√		√				226.1073	230.1325	
40	√		√		√		240.0979	244.1230	Also shown in the NNK study [a]
41	√	√	√		√		270.1234	274.1483	
42	√	√	√		√	√	272.1394	276.1645	
43	√		√		√		320.1030	324.1281	
44	√		√				327.0976	331.1227	
45			√		√		332.1493	336.1744	
46	√		√		√		355.1071	359.1322	

[a] See Dator R, et al. Anal. Chem. 2018, 90 (20), 11863–11872.